Investigation of the parameters of the plasma channel and dynamics of a microwave streamer in nitrogen and air

P. V. Vedenin

Moscow Radio-Engineering Institute, Russian Academy of Sciences, Moscow, Russia

N. A. Popov

Computational Center of the Russian Academy of Sciences, 117967 Moscow, Russia

(Submitted 27 March 1995)
Zh. Éksp. Teor. Fiz. **108**, 531–547 (August 1995)

A numerical model, which makes it possible to investigate the two-dimensional dynamics of plasma formation in a supercritical field in the electrostatic stage with a full set of plasma chemical reactions, is developed. The parameters of the plasma channel are determined and compared with experimental data. It is shown that propagation of a microwave streamer is accompanied by a self-consistent variation of the electron number density in the channel and its spatial dimensions so as to minimize the amplitude of the electric field at the center of the channel. The conditions for passage to the streamer mechanism of breakdown in self-sustained high-frequency high-pressure discharges are obtained. The distinguishing features of the streamer form of microwave discharges are discussed. © *1995 American Institute of Physics.*

1. INTRODUCTION

The possibilities of using high-pressure microwave discharges to remove freons from the atmosphere,[1–3] in electric-discharge plasma chemical reactors,[4,5] etc. have recently been investigated. The parameters and efficiency of the systems created are determined by the reduced electric field and the electron number density, as well as their distribution in the region where the source of electromagnetic radiation acts.

The overall picture of the development of a self-sustained high-pressure microwave discharge ($\nu_e \gg \omega$, where ν_e is the collision frequency of the electrons and ω is the oscillation frequency of the field), which was observed experimentally in Ref. 6–8, is qualitatively identical in different gases and can be broken down into the following stages: 1) the appearance of a quasispherical plasma cloud (plasmoid); 2) elongation of the plasmoid in the direction of the electric field $\mathbf{E}_0$ to a length comparable to the wavelength λ; 3) the appearance of one or more bright thin filaments parallel to $\mathbf{E}_0$; 4) growth of the filaments beyond the plasmoid, bending toward the incident radiation, and branching.

Stage 1 of the symmetric expansion of the quasispherical plasma cloud continues as long as it is transparent to the incident electromagnetic radiation, i.e., as long as the condition $|\varepsilon - 1| \ll 1$ holds, where ε is the dielectric constant of the plasma. The main processes in this stage are electron-impact ionization in the external electric field, attachment (for electronegative gases), and diffusion (at first free and then ambipolar). When the maximum plasma density reaches the value determined from the condition $|\varepsilon - 1| \simeq 1$, the influence of the space-charge field becomes significant.

As a result, the rate of expansion of the plasma cloud, which depends on the local values of the electric field strength, is found out to be greater in the polar regions than in the equatorial region. This is the reason for elongation of the plasmoid in the direction of the external field.[9,10] Based on the analogy to a similar phenomenon observed in a discharge in a static field, Gil'denburg *et al.*[10] called such an elongated plasmoid a microwave streamer.

Experimental studies of microwave discharges in supercritical fields obtained information on such parameters as the rate of elongation of the plasmoid v, the electron number density, and the temperature T_g of the gas in the streamer channel. According to the data in Ref. 7, the values of this rate in nitrogen at pressures $P = 20–50$ Torr were equal to $V = 4\times10^6$ to 10×10^6 cm/s, and the temperature of the gas reached a level of $T_g = 600–1000$ K. In air at $P = 760$ Torr, $V \lesssim 10^8$ cm/s and $T_g \simeq 7000$ K (Ref. 8).

Measurements of the electron number density in the channel of a microwave streamer have been performed in inert gases,[7,11] nitrogen,[7,12,13] and air.[14] The significant difference between the results obtained under similar experimental conditions should be noted. For example, in nitrogen at $P = 300–800$ Torr the electron number density was $N_e = 3\times10^{14}$ to 7×10^{14} cm^{-3} according to the data in Ref. 13 and $N_e > 3\times10^{16}$ cm^{-3} according to the data in Ref. 12. This disparity can be attributed to the conditions for the formation and subsequent dynamics of the discharges in those experiments.

For the most part, the contraction of microwave discharges was investigated theoretically and the experimental data enumerated were interpreted in terms of the thermal ionization instability (see the review in Ref. 6). The inadequacy of such an approach was pointed out in Refs. 5 and 9, where a streamer mechanism for the development of high-pressure microwave discharges was proposed.

The evolution of a plasmoid in the electrostatic stage, during which the effects associated with the finite value of the wavelength of the incident radiation can be neglected, was treated numerically in a planar two-dimensional approximation in Ref. 10. It was shown, in particular, that the amplitude of the field at the poles of the ellipsoid (and, therefore, its rate of elongation) is considerably smaller than that

 1063-7761/95/080286-10$10.00

which could have been expected on the basis of the familiar formula $|E_n|=|\varepsilon|\cdot|E_0|$ for a uniform plasma ellipsoid (see, for example, Ref. 15). Here E_n and E_0 are, respectively, the amplitudes of the fields at the poles and within the uniform ellipsoid.

In Ref. 16 the electrodynamic stage of the evolution of a microwave streamer until it reaches a size comparable to the wavelength was investigated along with the former stage. The important role of the electrostatic stage, which is characterized by rapid increases in the plasma concentration of the streamer and its rate of elongation, was demonstrated. Analytical relations for the spatial distribution of the electric field amplitude were obtained within a model of a nonuniform plasma ellipsoid. These relations made it possible to reveal the likely causes of the slowing and stopping of a microwave streamer in the nonelectrostatic stage.

Analysis of the results in Ref. 16 reveals that the space charge of the streamer channel predetermines the field strength in the region of the ionization wave front to a considerable extent. For this reason, an adequate description of the distribution and absolute values of the charged-particle density in the streamer channel has become especially important in the investigation of the dynamics of a microwave streamer. It should be noted that the most thorough investigations from the electrodynamic standpoint[10,16] were performed using simplified kinetic models.

The purpose of the present work was to devise a model which would make it possible to investigate the two-dimensional dynamics of plasma formation in a supercritical field in the electrostatic stage with a complete system of plasma chemical reactions, to determine the parameters of the plasma channel and compare them with experimental data, and to analyze the influence of those parameters on the dynamics of a microwave streamer.

2. DESCRIPTION OF THE MODEL

2.1. The evolution of the plasma cloud formed as a result of breakdown of the gas in a supercritical field of a linearly polarized electromagnetic wave is considered in the planar (x, y) two-dimensional approximation $(\partial/\partial z=0)$. The vector of the electric field of this wave $\mathbf{E}_v=\frac{1}{2}\mathbf{E}_v e^{-i\omega t}+\text{c.c.}$ is parallel to the y axis. The stage of symmetric diffusion-controlled expansion of a plasma from a filamentary seed center $N_e(t=0,\mathbf{r})=N_c\delta(x)\delta(y)$ [$\delta(\mathbf{r})$ is a delta function] continues, as already noted, as long as the condition $\sigma_*=4\pi\sigma/\omega\ll l$ holds, where σ is the conductivity of the plasma created (here N_c is the number of electrons per unit length of z). The distribution of the electron number density under these conditions has the form

$$N_e(t,r)=\frac{N_c\exp(-r^2/4Dt+\gamma_v t)}{4\pi Dt}, \qquad (1)$$

where $r^2=x^2+y^2$, $\gamma_v=\nu_i(E_v)-\nu_a$, D is the diffusion coefficient (the free diffusion coefficient D_e or the ambipolar diffusion coefficient D_a), and $\nu_i(E_v)$ and ν_a are, respectively, the frequencies of ionization by electron impact and of attachment in the field $\mathbf{E}_v$.

Since number densities in the range $N_e>3\times10^9$ cm^{-3}, which satisfy the condition $N_e(\partial N_e/\partial r)^{-1}\ll R_D$ (R_D is the Debye radius), occur in the initial stage, the coefficient $D=D_a$ corresponding to ambipolar diffusion should be plugged into Eq. (1). The diffusion becomes ambipolar when this inequality is reversed.

After a time $\tau_v=(20-30)/\gamma_v$ the plasma concentration increases so much that the space-charge field can no longer be neglected, and $4\pi\sigma/\omega>0.5$, holds symmetric expansion gives way to predominant elongation of the plasmoid along the direction of $\mathbf{E}_v$. It follows from the latter inequality that the value of the electron number density at which polarization of the plasma created begins to manifest itself increases linearly with the frequency of the field. For example, for $P\geqslant1$ atm and $\lambda\leqslant10$ cm, we have $N_e>3\times10^{13}$ cm^{-3}.

The results of the experiments in Refs. 7 and 8 and the numerical calculations in Refs 10 and 16 indicate that the plasmoid streamer is nearly ellipsoidal, especially in the electrostatic stage. This allows us to advance the following important hypothesis: the spatial distribution of the electron number density does not vary during the entire computation time and has the form

$$N_e(t)=N_e^0(t)f[r_*,S_k(t)], \quad k=1-m. \qquad (2)$$

Here we have written $x_*=x/l_x(t)$, $y_*=y/l_y(t)$, and $r_*^2=x_*^2+y_*^2$, where $l_y(t)$ and $l_x(t)$ are respectively, the major and minor semiaxes of the plasma ellipsoid, f is a given function which satisfies the conditions $0\leqslant f\leqslant1$ and $f(\infty)=0$, and the S_k $(k=1,\cdots,m)$ are parameters which specify the shape of the plasmoid (as m increases, the profile of f becomes sharper). Basing the model on Eq. (2), we must subsequently describe the distribution of the electric fields along the x and y axes and the evolution of the parameters $l_x(t)$, $l_y(t)$, $N_e^0(t)$, and $S_k(t)$.

The appearance of electrons outside the plasma zone is associated with a diffusion process. Their number density then increases as a result of ionization in the external field. This model of the propagation of a breakdown wave is applicable to any composition of the gas mixture (unlike, for example, the photoionization model) and, in this sense, is more universal.

The velocity of the breakdown wave front in the X and Y directions was determined from an asymptotic $(t\to\infty)$ solution of the Kolmogorov–Petroskiĭ–Piskunov equation[17] (under the assumption that the wave moves independently in these directions). To take into account the deviation of the current value of the velocity from its asymptotic value, a multiplier q was introduced into this solution. As the calculations in Ref. 16 showed, we have $q_x\simeq1$, $q_y=1-2$, and the rates of elongation and broadening of the plasmoid are related to the values of the reduced electric fields $|E_n|/N$ and $|E_t|/N$ at the points $(0,\pm l_y)$ and $(\pm l_x,0)$ by the following expressions

$$dl_y/dt=2q_y\sqrt{D_a\gamma(E_n/N)\theta(\gamma)},$$
$$dl_x/dt=2q_x\sqrt{D_a\gamma(E_t/N)\theta(\gamma)}, \qquad (3)$$

where $\Theta(\gamma)$ is a Heaviside function.

Utilization of the technique proposed in Ref. 16 made it possible to obtain expressions for the distribution of the amplitude of the electric field on the X and Y axes:

$$\frac{E_{1,2}}{E_0}=\frac{1}{\varepsilon}\left[1+\frac{i\sigma_*}{L^2-1}(fL^2-1-LI_{1,2})\right],$$

$$E_0=\frac{E_v}{1+i\sigma_*/(L+1)}, \tag{4}$$

where

$$E_0=E(0,0),\quad E_1=E(x_*,0),\quad E_2=E(0,y_*),$$

$$\varepsilon=1+if\sigma_*,\quad \sigma_*=\frac{4\pi\sigma_m}{\omega},\quad \sigma_m=\frac{e^2N_e^0}{m\nu_e},$$

$$L=\frac{l_y}{l_x},\quad I_{1,2}=\int_0^{r_*}\frac{d\eta f'(\eta)}{\sqrt{1+\alpha_{1,2}\eta^2}},$$

$$\alpha_1=\frac{L^2-1}{x_*^2},\quad \alpha_2=-\frac{L^2-1}{L^2y_*^2}.$$

The following conclusions can be drawn from the relations (4).

1. When the plasma is distributed uniformly within the streamer $[-f'=\delta(r_*-1)]$, the expressions (4) transform into the well-known equations[15]

$$E(x_*\leqslant 1,0)=E(0,y<1)=E_0,\quad E(0,1)=\varepsilon_0E_0$$

$$E_0=\frac{E_v}{1+\dfrac{\varepsilon_0-1}{L+1}},\quad \varepsilon_0=1+i\sigma_*.$$

2. Under the condition

$$\left|\frac{d^2f}{dr_*^2}\right|\ll L^2 \tag{5}$$

the expression for $E(x_*,0)$ can be rewritten in the form

$$E(x_*,0)=E_0[1+O(\sigma_*/L^2)]. \tag{6}$$

According to Refs. 10 and 16, the following inequalities hold in the electrostatic stage of streamer elongation

$$\sigma_*^2\ll 1,\quad L\simeq 1,\quad \sigma_*^2/L^2\lesssim 1,\quad L^2\gg 1.$$

Therefore, when condition (5) holds, we have

$$E(x_*\leqslant 1,0)\simeq E_0. \tag{7}$$

The electron number density profile was chosen in the following form:

$$f(x_*,y_*,t)=\begin{cases}1, & S_0(t)\leqslant S\leqslant 1,\\ S/S_0(t), & 0\leqslant S\leqslant S_0(t),\\ 0, & S(t)<0,\end{cases} \tag{8}$$

where $S=1-x_*^2-y_*^2$. This profile takes into account the characteristic thickness of the ionization wave function in the direction of $\mathbf{E}_v$

$$\Delta_y=l_y(1-\sqrt{1-s_0}) \tag{9}$$

and depends only on three parameters $l_x(t)$, $l_y(t)$, and $S_0(t)$. In addition, the distributions of the amplitude of the field in the X and Y directions corresponding to (8) are consistent with the results of the calculations in Ref. 16. We note that for $L^2\gg 1$, the calculated[16] and model profiles of the electron number density along the x axis differ appreciably. However, since $\sigma_*/L^2\ll 1$ holds in this case, this disparity can be disregarded in accordance with (6).

When (8) is taken into account, the expression for the amplitude of the field at the poles of the plasmoid becomes

$$E_y(0,\pm 1)\simeq E_0\cdot\begin{cases}1+1\sigma_*\sqrt{\dfrac{2r_c}{\Delta_y}}, & r_c\ll\Delta_y, \quad (10a)\\ \varepsilon_0, & r_c\gg\Delta_y, \quad (10b)\end{cases}$$

where $r_c=l_x^2/l_y$ is the radius of curvature at these points. It follows from (10), in particular, that when the condition $r_c\ll\Delta_y$ holds, the field at the head is enhanced considerably less than in the case of a uniform plasma ellipsoid.

An analysis of the results of the calculations in Refs. 10 and 16 reveals that the width of the front Δ_y remains approximately constant and equal to the radius of the plasmoid R_0 at the end of symmetric expansion throughout nearly the entire electrostatic stage of plasmoid elongation. When (9) is taken into account, this allows us to write the expression for $S_0(t)$

$$S_0(t)=\frac{R_0}{l_y(t)}\left[2-\frac{R_0}{l_y(t)}\right]. \tag{11}$$

Thus, within the model defined by (3) and (8), the spatial distribution of the electron number density can be described for an assigned value of $N_e^0(t)$ by solving Eqs. (2) and (11) for dl_y/dt, dl_x/dt and $S_0(t)$. The model developed is completed by the system of equations of the plasma chemical kinetics for determining $N_e^0(t)$ in the central portion of the streamer, where the field equals E_0.

A plasma conductivity $\sigma_*^0=4\pi\sigma^0/\omega=0.5$, which corresponds to the electron number density $N_e(0)$, was assigned at the initial moment in time. Such a number density is generated after a time τ_v during symmetric expansion of the plasma cloud. At this point the radius of the plasmoid reaches a value equal to $R(\tau_v)\simeq 3\sqrt{D_a\tau_v}$, which was selected as the initial condition $R_0=R(\tau_v)$. The value of $R(\tau_v)$ is determined by the radial coordinate at which the electron number density at the center $N_e(\mathbf{r}=0)$ decreases by a factor of e^2 according to (1).

2.2. In describing the plasma chemical processes we assumed that under these conditions the molecules in a discharge are excited and ionized predominantly by electron impact from the ground state and that the rates of these processes depend only on the local values of the reduced electric field E/N. The corresponding dependences for $E/N<300$ Td for nitrogen and air were taken from Refs. 18 and 19. The ionization constants for these gases at high values of E/N were borrowed from Ref. 20. The influence of secondary collisions with vibrationally excited molecules was taken into account according to Ref. 21

$$\log(k(T_v)/k(T_0))=B\exp(-h\omega/kT_v)/(E/N)^2,$$

where $h\omega$ is the vibrational quantum of a molecule and T_v is the vibrational temperature. It should be noted that the data in Refs. 18 and 19 were obtained for discharges in a constant electric field. However, several investigations (see the review in Ref. 21) it revealed that in the range of values $\nu_e/\omega\gg 1$

the use of these data for microwave discharges is reasonable when the effective frequency of collisions of electrons with molecules is properly chosen.

In the present work the possible variation of the ionization and excitation frequencies of the molecules due to e–e processes was not taken into account [even though in high-pressure microwave discharges there are regions with a high concentration $N_e/N > 10^{-4}$–10^{-3} (see Refs. 11–14)]. As was noted in Ref. 21, in molecular gases the variation of the frequencies of the ionization and excitation of molecules due to e–e processes is relatively small up to $N_e/N \geqslant 10^{-3}$. This is attributed to the low-threshold excitation of vibrational levels and makes it possible to disregard the influence of these processes in a first approximation.

The reactions involving charged particles were described with consideration of the following eight kinds of positive and negative ions: O_2^+, O_4^+, N_4^+, NO^+, O^-, O_2^-, O_3^-, O_4^-. Under these conditions the predominant processes are the bulk formation and destruction of these particles. The system of ion–molecule reactions in Ref. 22 was chosen as a base.

The dynamics of the neutral components of a nitrogen–oxygen mixture was described by a system of balance equations for the concentrations of $N(^4S)$, $N_2(A^3\Sigma_u)$, $N_2(C^3\Pi_u)$, $N_2(B^3\Pi_g$, $B'^3\Sigma_u$, $W^3\Delta_u)$, $N_2(a^1\Pi_g, a'^1\Sigma_u$, $w^1\Delta_u)$, NO, $N(^2D)$, $O(^3P)$, $O(^1D)$, $O(^1S)$, $O_2(a^1\Delta_g)$, $O_2(b^1\Sigma_g)$, and O_3, as well as by equations for the temperature of the gas and the vibrational temperatures of N_2, O_2, and O_3. A detailed description of the kinetic scheme and the results of test calculations for nitrogen with small additions of oxygen and air were presented in Refs. 23 and 24, respectively.

The possibility of the effective destruction of negative ions on $O(^3P)$ atoms, which form upon the dissociation of O_2 by electron impact and in reactions involving the quenching of electronically excited nitrogen molecules by oxygen, is noteworthy.

The local time-dependent balance equations were solved for all the components listed above. In particular, the equation for the number density of electrons, whose formation is most significant in the present work, has the following form:

$$\partial N_e/\partial t = N_e(\nu_i - \nu_a) + Q_{\text{as}} - N_e[O_2^+ + O_4^+]\beta$$
$$- N_e[O_2]^2 k_a + [O(^3P)]k_{\text{det}}[O^- + O_2^-],$$

where k_a, $\beta_{1,2}$, and k_{det} are, respectively, the constants for three-particle attachment, electron–ion recombination, and detachment on $O(^3P)$ atoms. The term Q_{as} describes the increase in the electron number density in associative ionization reactions.[23,24] It should be noted that when the above system of plasma chemical reactions is included, the distribution of the electron number density along the streamer channel should correspond more closely to the profile (8) than the results of the calculations in Ref. 16.

3. RESULTS OF THE CALCULATIONS AND DISCUSSION

Figure 1 presents the results of a comparison of the data from the full-scale numerical simulation in Ref. 16 and test calculations based on the electrostatic model described above

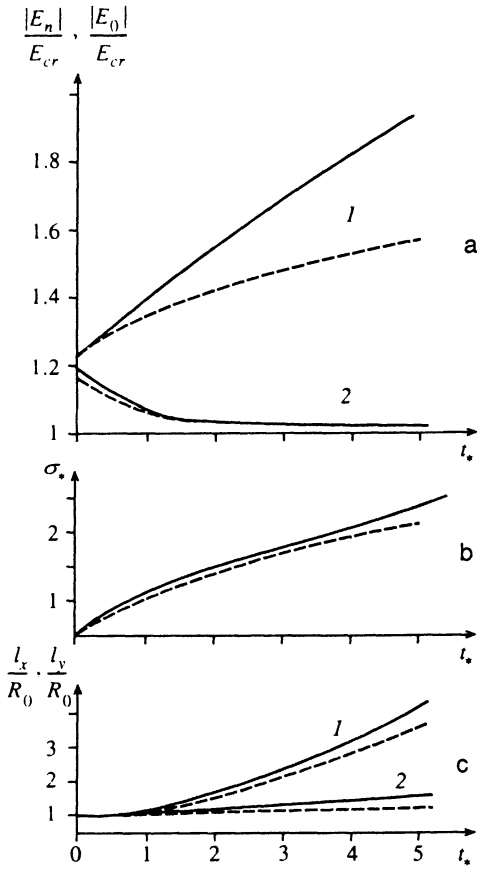

FIG. 1. Time dependences of a) $|E_y|/E_{\text{cr}}$ (*1*) and $|E_0|/E$ (*2*), b) σ_*, and c) l_y/R_0 (*1*) and l_x/R_0 (*2*) obtained in Ref. 16 (solid line) and in the present work (dashed line). $E_v/E_{\text{Cr}} = 1.2$, $\nu_e/\omega = 70$, $q_y = 1.5$.

(but with the use of a simplified kinetic scheme in which only ionization, attachment, and one kind of ion with an effective electron–ion recombination coefficient β were taken into account). As in Ref. 16, for σ_* we wrote the equation

$$\frac{d\sigma_*}{dt_*} = \sigma_* \left(\left| \frac{E_0}{E_{\text{cr}}} \right|^{5.3} - 1 \right) - \beta_* \sigma_*^2, \tag{12}$$

where $t_* = t\nu_a$, $\nu_a = \text{const}$, E_{cr} is the breakdown field, and $\beta_* = \beta m \nu_e \omega / 4\pi e^2 \nu_a$.

The calculations were performed for the following conditions:

$$\frac{E_v}{E_{\text{cr}}} = 1.2, \quad \frac{\nu_e}{\omega} = 70, \quad q_y = 1.5, \quad q_x = 1.$$

The maximum relative difference between the calculated values in the present work and in Ref. 16 to 20% and is observed when $t_* \simeq 5$. In the analogous calculations with $E_v/E_{\text{cr}} = 1.05$, $\beta_* = 0$, and $\beta_* = 10$ this difference was already appreciably smaller.

Note that for $t_* \geqslant 1.5$, the amplitude of the field at the center of the plasmoid E_0 remains quasisteady value. The cause of this behavior of E_0 is illustrated by the following scheme:

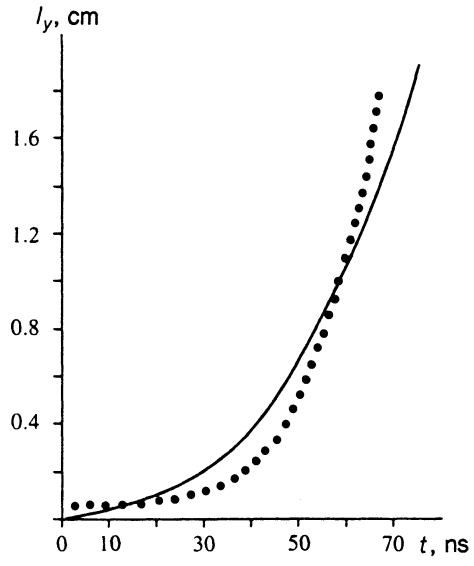

FIG. 2. Dynamics of the elongation of a microwave streamer $l_y(t)$ in the direction of the external field for the conditions of the experiment in Ref. 8: air, $P=760$ Torr, $\lambda=8.5$ cm, $E_v/N=160$ Td, $\tau_{pul}=70$ ns; (●) — data from 8; $\gamma_v\tau_v=25$, $q_y=1.5$.

$$\frac{\sigma_*}{L}\uparrow\rightarrow\begin{array}{l}\nearrow\ |E_0|\downarrow\rightarrow\sigma_*\downarrow\\ \searrow\ |E_y|\uparrow\rightarrow\dfrac{dl_y}{dt}\uparrow\end{array}\begin{array}{l}\searrow\\ \nearrow\end{array}\frac{\sigma_*}{L}\downarrow. \tag{13}$$

Acccording to Eqs. (4) and (12), as $\sigma_* L$ increases the field E_0 in the center of the plasmoid and the quantity σ_* decrease. At the same time the field amplitude E_n at the head of the streamer increases [cf. Eqs. (10a) and (9)] and the rate of elongation i_y grows. This causes a drop in σ_*/L.

We recall that, according to (4), at a fixed value of the external field the value of E_0 is determined completely by σ_*/L, which, as is seen from (13), becomes quasisteady after a certain time.

According to the scheme (13), the values of the stationary field E_0^s depend on the specific form of the functions $\sigma_*(E_0)$ and $i_y(E_y)$, which, in turn, are determined by the kind of gas, the system of kinetic equations considered, etc. The results which were obtained using the system of plasma chemical reactions in Sec. 2.2 and describe the breakdown of nitrogen ($P=15$–50 Torr) and air ($P=760$ Torr) in a field of microwave radiation with the parameters from Refs. 7 and 8, respectively, are presented next.

Figure 2 presents the calculated and experimental data on the dynamics of the elongation of a microwave streamer $l_y(t)$ parallel to the external field for the conditions in Ref. 8: air, $P=760$ Torr, $E_v/N=160$ Td, $\tau_{pul}=70$ ns, $\lambda=8.5$ cm. We note that the total pulse duration also includes the stage of symmetric expansion of the plasma cloud; therefore, $\tau_{pul}^{exp}=t_v+\tau_{pul}$. The experimental data on the plasmoid length $l_y(t)$ were obtained by photographing the emission from the region of the streamer channel. Since the time between the moment when the microwave generator is turned on and the appearance of emission under the conditions in

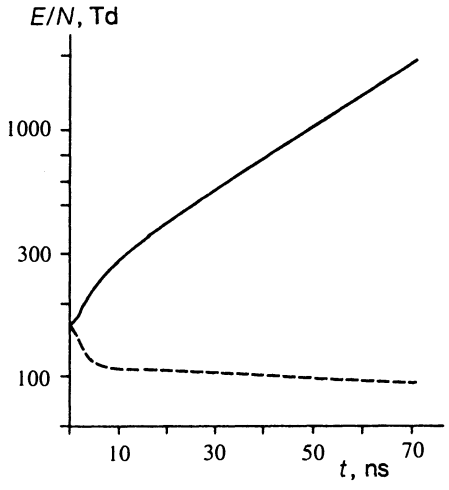

FIG. 3. Dependence of the reduced electric field at the poles $|E_y|/N$ (solid line) and the reduced electric field at the center of the plasmoid $|E_0|/N$ (dashed line) on the time for the conditions in Fig. 2.

Ref. 8 can vary appreciably from experiment to experiment, to compare the experimental data with the results of the calculations the corresponding plots of $l_y(t)$ were matched in the region where they vary rapidly, i.e., at $l_y=1\pm0.1$ cm. The calculated value of the rate of elongation of the plasmoid in the direction parallel to the external field at $t>65$ ns exceeds 6×10^7 cm/s (in the experiments in Ref. 8 $v_{max}\simeq10^8$ cm/s).

The transverse dimension of the streamer channel $l_x(t)$ during a pulse varied slightly from $R_0\simeq0.1$ mm (the initial radius of the plasma cloud) to $l_x^{max}\simeq0.25$ mm. Note that according to Ref. 8, the transverse dimension of the plasmoid reaches a value of $r=2$ mm, which greatly exceeds l_x^{max}. In our opinion, this may happen because the ionizing radiation from the streamer channel creates a plasma corona around it, whose emission is detected in the experiments under consideration. The cross section for the absorption of radiation with $\lambda<105$ nm by oxygen molecules is $\sigma\simeq10^{18}$ cm^2 (Ref. 25), and the characteristic absorption length equals $l_f=(\sigma[O_2])^{-1}=1.8$ mm, in agreement with the data in Ref. 8.

In powerful gas discharges highly excited oxygen atoms can serve as a source of ionizing radiation.[26] We evaluated the intensity of the emission of the $O(3d^3D-2p^3P)$ electronic transition (the wavelength is $\lambda=102.7$ nm). The cross section for excitation of the $O(3d^3D)$ state by electron impact was borrowed from Ref. 27. The inclusion of this photoionization mechanism in the treatment makes it possible to produce additional plasma with an electron number density $N_e<10^{12}$ cm^{-3} at distances less than l_f.

Figure 3 shows plots of the time dependence of the reduced electric fields at the poles ($|E_n|/N$) and at the center of the plasmoid ($|E_0|/N$). In the final stage of growth of the plasmoid, the field gain reached a value of $|E_n|/|E_0|>30$. As the amplitude of E_y increases, the ionization frequency ν_i at the head of the streamer increases sharply. For $|E_n|/N>450$–500 Td, ν_i exceeds the field frequency ω. As we know, when the frequency of inelastic collisions of the

electrons is $\nu_c \gg \omega$ and the rate constants of the ionization and excitation processes depend strongly on E/N, the use of values of E/N which are averaged over the oscillation period to determine these constants can lead to large errors, and the oscillatory character of the field must be taken into account. In the case of microwave discharges, the condition $\nu_i(T_e) \ll \omega$ holds at a sufficiently high electron energy ($T_e \geqslant 4.5$–5 eV), which is comparable to the ionization potential of the molecules in the mixture. At such values of T_e the plot of $k_i(E/N)$ is nearly linear,[20] and describing the ionization process in terms of a mean field does not lead to appreciable errors.

Note that in the region where $\nu_i \gg \omega$ the gradients of the electric field strength and the gradients of the electron energy are large. To validate the possibility of using the local dependence of T_e on E/N in this region, we refer to the results in Ref. 28, where it was shown that nonlocal effects are displayed in a fairly small vicinity of the streamer head (at distances less than 2–3 times the radius of the head) and do not have an appreciable influence on the propagation rate of the streamer or on the parameters of the plasma channel.

In addition, the appearance of a high-field region ($\nu_i \gg \omega$) at the streamer head can cause the value of $E_n(t)$ to differ from (4), since the assumption regarding the slow variation of the field amplitude during an oscillation period ($\partial/\partial t \to -i\omega$) used to derive the relations (4) does not hold when $\nu_i \gg \omega$. However, as the evaluations performed showed, the size of this region is relatively small ($\ll \Delta_y^2$); therefore, the field amplitude $|E_y|$ is determined mainly by the space charge of the part of the streamer where $\nu_i < \omega$ holds and can thus be calculated from Eq. (4).

Figure 4 presents calculations of the dynamics of the main components of a 4:1 N_2:O_2 mixture excited by a microwave discharge.[8] As a result of the intense dissociation of the oxygen molecules, the degree of O_2 dissociation reached 20–25%. This determines the features of the further evolution of the mixture under consideration, particularly the effective destruction of the negative ions in reactions involving $O(^3P)$ atoms.

In the initial stage of burning of the discharge ($t = 10$–40 ns), when the field within the plasmoid is $E_0/N \geqslant 100$ Td (Fig. 2), there is a rapid [relative to $N_e(t)$] increase in the concentration of negative ions [$O^- + O_2^-$] (Fig. 4), which is compensated mainly by the destruction of the latter on $O(^3P)$ atoms. Since the concentration $[O(^3P)]$ is high under the conditions under consideration, the contribution of the negative ions to the total balance of charged particles is less than 20% in all stages of the calculation.

In addition, under the conditions considered here an important role is played by associative ionization processes involving excited oxygen atoms[23,24]

$$O(^1S)+O(^1S) \to O_2^+ + e, \quad O(^4S)+O(^1S) \to NO^+ + e,$$

$$k \simeq 3\times 10^{-11}\ \text{cm}^3/\text{s}. \qquad (14)$$

The main reactions resulting in the formation and destruction of $O(^1S)$ atoms are

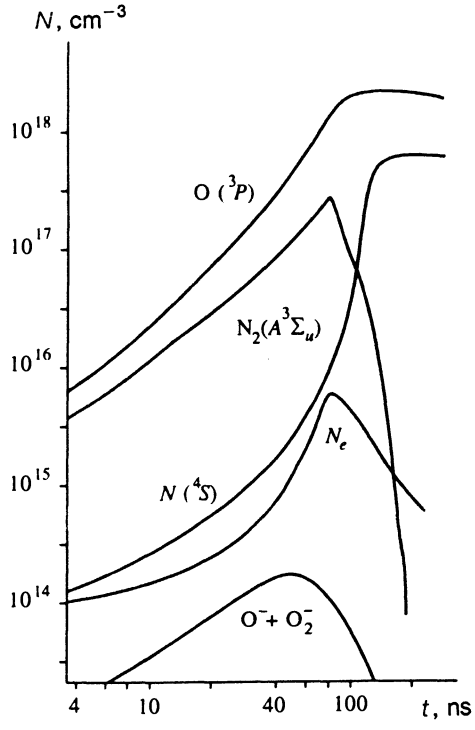

FIG. 4. Results of calculations of the dynamics of the principal components of a 4:1 N_2:O_2 mixture excited by a microwave discharge.[8]

$$N_2(A^3\Sigma_u)+O(^3P) \to N_2(v)+O(^1S),$$

$$k = 2.8\times 10^{-11}\ \text{cm}^3/\text{s},$$

$$O(^1S)+O_2 \to O(^3P,{}^1D)+O_2(v),$$

$$k = 4\times 10^{-12}\exp(-870/T)\ \text{cm}^3/\text{s},$$

$$O(^1S)+O(^3P) \to O(^3P,{}^1D)+O(^3P),$$

$$k = 5\times 10^{-11}\exp(-310/T)\ \text{cm}^3/\text{s}.$$

The complete system of processes involved in the formation and quenching of $O(^1S)$ in nitrogen–oxygen mixtures was presented in Ref. 24.

Under the conditions considered here the charged particles are generated mainly in the streamer channel in associative ionization reactions at $t \geqslant 25$–30 ns. Thus, as the concentration of $O(^1S)$ atoms increases, $N_e(t)$ increases due to the reactions (14), which, in turn, causes an additional increase in the concentration of $O(^1S)$. This is why the derivative $\partial N_e/\partial t$ increases with time. This tendency for an increase in the electron number density is apparently maintained until there is an appreciable decrease in the electric field strength at the center of the channel.

If the associative ionization processes are not taken into account, the values of the electron number density in the streamer channel are found to be strongly underestimated, and the rate of elongation of the latter decreases as a result. For example, Grachev *et al.*[8] theorethically estimated the maximum electron number density as: $N_e^{\max} \leqslant 4.6\times 10^{14}$ cm^{-3}, which is approximately an order of magnitude lower than the values we obtained including the associative ioniza-

tion processes. In addition, if $N_e^{max} \leq 4.6\times10^{14}$ cm^{-3} holds, then, according to (3) and (4), the streamer velocity is less than 10^7 cm/s, which is significantly smaller than the measured values (Fig. 2).

Rapid decay of the emission was noted in Ref. 8 after the streamer achieved a length $l_y \simeq \lambda/2\pi$ (during the time τ_{pul}). This can be associated with the mismatching of the cavity to the microwave generator, which occurs after breakdown of the gas and is recorded by the cavity field amplitude detector. It was postulated on the basis of these data that $E_v = 0$ at times greater than τ_{pul}.

The results of the calculations of the evolution of the composition of the mixture in the postdischarge period (Fig. 4) attest to an appreciable increase in the concentration of $N(^4S)$ atoms. This is attributed to occurrence of the reaction

$$O(^3P)+N_2 \rightarrow N(^4S)+NO, \qquad (15)$$

whose rate increases significantly as the the high vibrational levels of the nitrogen molecules further populated. Reaction (15) and the subsequent oxidation of the $N(^4S)$ atoms results in the vigorous formation of nitrogen oxides, whose concentration reaches the value [NO] = 10^{18} cm^{-3}.

The increase in the gas temperature in the discharge stage is associated mainly with the occurrence of the reaction

$$O(^1D)+N_2 \rightarrow O(^3P)+N_2(v)+\Delta T_g,$$
$$k = 2\times10^{-11}-2.5[m1]0^{-11}\text{cm}^3/\text{s},$$

in which up to 70% of the $O(^1D)$ excitation energy is utilized to heat the mixture.[24] Metastable $O(^1D)$ atoms can form as a result of the dissociation of oxygen via the $O_2(B^3\Sigma_u)$ state, which is populated from the ground state by electron impact, and in reactions involving the quenching of electronically excited $N_2(B^3\Pi_g,\ B'^3\Sigma_u,\ w^3\Delta_u)$ and $N_2(a^1\Pi_g,\ a'^1\Sigma_u,\ w^1\Delta_u)$ molecules. The density of $O(^1D)$ at the end of pulse is equal to 6×10^{16} to 8×10^{16} cm^{-3}. The temperature of the gas in the discharge stage less than 100–150 K, while the total amount of energy supplied to the streamer channel during a pulse can be as high as $\simeq$0.9 eV/molecule.

In the postdischarge period the VT relaxation reaction of N_2(vib) on oxygen atoms causes an sharp temperature rise, which is accompanied by gas-dynamic expansion of the channel at times $t > \tau_g \sim l_x/C_s$ (C_s is the velocity of sound). Since the heating of the gas occurs mainly in the streamer channel and since the temperature in the plasma corona varies relatively little, we have $l_x < 0.2$ mm and $\tau_g \sim 0.7$ μs.

Figure 5 presents experimental data and the results of the calculations of the dependence of the rate of elongation of the plasmoid on the gas pressure for the following conditions:[7] nitrogen, $P = 15$–50 Torr, $E_v = 2.1$ kV/cm, $\tau_{pul} = 1$–15 μs, $\lambda = 4$ cm. The pulse duration, which was determined during the calculations from the condition of applicability of the electrostatic approximation $2l_y(t) < \lambda/\pi$, was equal to 350–450 ns. As the pressure increases and the value of E_v/N decreases, the ionization frequency and, accordingly, the rate of elongation of the streamer decrease.

The transverse dimension of the plasmoid $l_x(t)$ varied by a factor of about 1.4 during a computational pulse. At the same time, the ratio l_y/l_x reached values of 4–4.6 for all the pressures considered, in agreement with the experimental data in Ref. 7.

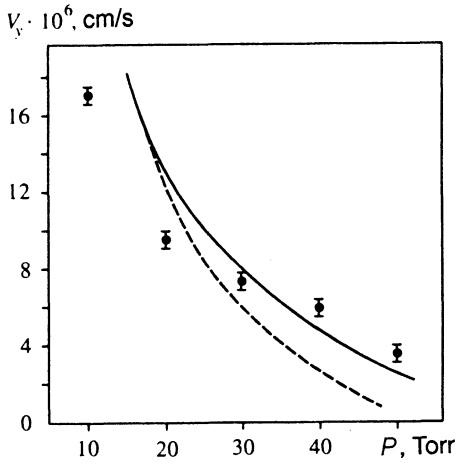

FIG. 5. Dependence of the rate of elongation of the plasmoid on the nitrogen pressure for the conditions in Ref. 7: $E_v = 2.1$ kV/cm, $\lambda = 4$ cm. ● – experimental data from Ref. 7; solid line, dashed line – results of calculations with and without consideration of the associative ionization reactions, respectively.

Figure 6 presents plots of the time dependence of the reduced electric fields at the poles and in the center of the plasmoid (a), as well as the main components of a nitrogen plasma (b) excited by a microwave discharge.

The important role of the associative ionization reaction[23]

$$N_2(a'^1\Sigma_u)+N_2(a'^1\Sigma_u) \rightarrow N_4^+ + e, \quad k = 2\times10^{-10}\text{cm}^3/\text{s}, \qquad (16)$$

which results in an increase in the ionization frequency ν_i at the center of the plasmoid at the end of the computational pulse, when $|E_0|/N$ decreases to 80–100 Td, should be noted. As ν_i increases, the rate of elongation of the plasmoid also increases (solid curve in Fig. 5). The associative ionization reactions become more important as the pressure increases, since the reduced electric field at the center of the plasmoid decreases and the ratio of the impact ionization frequency to the excitation frequency of the singlet nitrogen states participating in reaction (16) decreases as a result.

The amount of energy supplied to the streamer channel during the computational pulse is equal to 0.1 eV/molecule, most of the energy being released not in the initial stage ($t < 50$ ns), when the value of E_0/N is relatively high, but later on, when $E_0/N \leq 130$ Td (see Fig. 6a). At this point the electron number density in the channel exceeds $N_e > 10^{13}$ cm^{-3} (Fig. 6b). A similar situation is observed in air (Figs. 3 and 4), where most of the energy is released at $E_0/N \simeq 85$–90 Td and the electron number density reaches $N_e > 10^{15}$ cm^{-3}. These circumstances should be taken into account in analyzing the possibility of using the streamer form of microwave discharges in supercritical fields for plasma chemistry and other applications.

Let us comment on the conditions for the existence of the streamer form of discharges in wave fields. The criterion

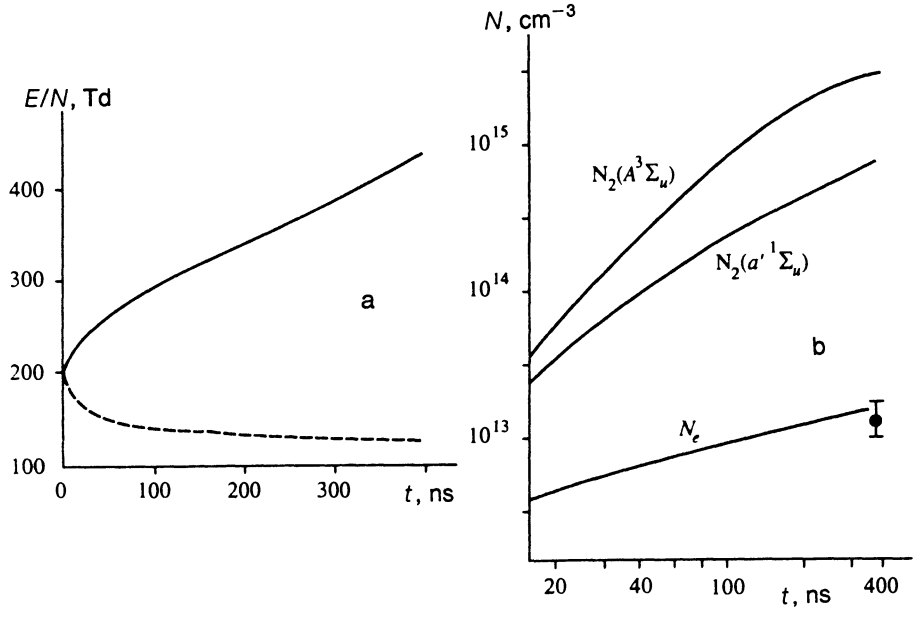

FIG. 6. Time dependences of the reduced electric field $|E_y|/N$ at the poles (solid line) and the reduced electric field at $|E_0|/N$ the center of the plasmoid (dashed line) (a) and of the principal components of a nitrogen plasma (b). For the conditions, see Fig. 5. ● – experimental data from Ref. 7; $P=30$ Torr.

for passage from the Townsend mechanism of breakdown to the streamer mechanism is that the field of the space charge equal the external field E_v. At fixed values of E_v and P the time needed to produce the required number density N_e^* in stationary fields is bounded by $\tau_*=d/V_{dr}(E_v)$, where d is the distance between the electrodes, V_{dr} is the drift velocity of the electrons, and the corresponding condition (Meek's criterion) can be written in the form

$$\nu_i d/V_{dr}\geqslant 20-30.$$

In wave fields the restriction placed on the value of τ_* is attributed to the fact that the dimensions of the plasmoid cannot exceed the wavelength λ (see, for example, Ref. 16 and the experimental data in Refs. 6–8), i.e., $2R(\tau_*) \leqslant \lambda$. This inequality (with consideration of the criterion $\nu_i\tau_* \geqslant 20-30$) is equivalent to the relation

$$\nu_i\lambda^2/D_a\geqslant 1000-1500 \tag{17}$$

or

$$\lambda P\ [\text{cm}\cdot\text{Torr}]\geqslant 5\times 10^3\cdot(\nu_i^v\ [\text{s}^{-1}])^{-0.5}$$

(ν_i^v is the ionization frequency in the field E_v at $P=1$ Torr), which specify the condition for passage to the streamer mechanism of breakdown in self-sustained high-frequency high-pressure discharges.

We note, however, that as the wavelength increases, the minimum area of the focal spot increases as λ^2; therefore, the creation of supercritical fields at the focus of the beam requires

$$\lambda P\ [\text{cm}\cdot\text{Torr}]\leqslant 0.3\sqrt{W}, \tag{18}$$

where W is the power of the radiation source in watts. It should be acknowledged that the microwave range is optimal for simultaneously satisfying the conditions (17) and (18), since the inequality (18) can be difficult to satisfy in hf high-pressure discharges and (17) is generally violated in the optical frequency range.

The results of the calculations performed allow us to advance several hypotheses, which have a fairly general character.

1. The model of a uniform plasma ellipsoid $\Delta_y \ll r_c$ is not applicable during the development of a high-frequency streamer. It follows from our calculations, as well as the data in Ref. 16 that $\Delta_y/r_c=\Delta_y L/l_x\gg 1$. The latter is especially important, since the parameters of a microwave streamer are often evaluated on the basis of just that model (see Refs. 8, 9, etc.), which can overestimate $|E_n|/N$ by a factor of 20 or more [see the expressions (10a and 10b)] and, accordingly, to significant overestimation of the rate of elongation of the streamer.

It was postulated in Refs. 7,8,12,13 and elsewhere that the field within a plasmoid E_0 is equal to the incident field E_v. However, as is seen from Figs. 3 and 6, the polarization of the plasma created produces a significant difference between E_0 and E_v.

2. One of the main characteristics influencing the dynamics of a microwave streamer is the parameter σ_*/L, which determines the amplitude of E_0 at the center of the plasmoid [see (4) in the limit $L\gg l$]. As we have already noted, this is a consequence of the fact that σ_*/L and E_0 reach stationary values at these times [see (13)].

How σ_*/L approaches a stationary value varies as a function of the initial conditions. When $\sigma_*^0<0.5$, σ_*/L increases to a steady value as the electron number density increases (at a practically constant value of $L=l_y/l_x=1$). When $\sigma_*^0>0.5$, rapid elongation of the streamer and an increase in L occur as E_y increases. In contrast same time, when the value of σ_*^0 is overestimated, the rate of the increase in $N_e(t)$ is small, since the field E_0 decays rapidly. As a result, σ_*/L decreases from its initial value to a steady value.

From this information [as well as the scheme (13)], it can be concluded that the self-organization of a microwave streamer occurs in such a manner that the amplitude of the

field E_0 at the center of the plasmoid varies as little as possible.

3. An important parameter, which determines the strength of the field at the head of the streamer, its rate of elongation, etc., is the product of the electron number density in the ionization wave and the time $N_e\tau_e$ for polarization of the plasma at the head of the streamer. Unlike discharges in a static field, where $\tau_e \sim \nu_i^{-1}$ holds (Refs. 29 and 30), in high-frequency fields there is a new characteristic time ω^{-1}, and $\tau_e = \min(\nu_i^{-1}, \omega^{-1})$. In microwave fields we have $\tau_e \sim \omega^{-1}$, and the field gain at the head is determined by the value of $4\pi\sigma/\omega > 1$ (see, for example, Refs. 5 and 6). Thus, the electron number density and the release of energy in the streamer channel can be regulated within certain ranges by varying the frequency ω. This may turn out to be important for applications. When the frequency of the field is high, a high value of N_e is needed for the streamer to move. This accounts for the relatively large (compared with the values in a stationary electric field)[1)] values of the degree of ionization $N_e/N > 10^{-4}-10^{-3}$ which were obtained in our calculations and observed experimentally in Refs. 11–14 in fields in the microwave range.

4. CONCLUSIONS

A numerical model has been developed, which makes it possible to investigate the two-dimensional (planar) dynamics of plasma formation in a supercritical field in the electrostatic stage with a sufficiently complete system of plasma chemical reactions. Calculations have been performed of the evolution of a microwave streamer from diffusion-controlled plasma formation to a plasmoid extended along the electric field with a length $2l_y$ comparable to the half-length of the electromagnetic wave. Rates of elongation of the streamer and parameters of the plasma channel have been obtained in nitrogen and air, which are consistent with the available experimental data.

It has been shown that under the conditions considered the space charge of the streamer channel influences the electric field strength in the region of the ionization wave front to a considerably greater degree than does the charge of the head. This calls for a fairly complete description of the processes which determine the distribution of the electron number density in the channel. For example, consideration of the reactions involving the dissociation of negative ions into oxygen atoms and associative ionization processes, which cause a significant increase in the conductivity of the plasma channel and its rate of elongation, turned out to be very important for discharges in air. These processes cause a significant increase in the conductivity of the plasma channel and its rate of elongation.

The conditions for passage to the streamer mechanism of breakdown in self-sustained high-frequency high-pressure discharges have been obtained. It has been shown that the microwave range is optimal for satisfying these conditions.

One distinctive feature of a high-pressure microwave streamer is the fact that the amplitude of the electric field at its head and, therefore, its rate of elongation depend not only on the value of the electron number density (as in a static field), but also on the frequency of the field ω or, more precisely, on their ratio $\sigma_* = 4\pi\sigma/\omega$. This makes it possible to remove the restriction on the peak electron number density in the streamer channel (which exists in static fields)[29,30] due to the increase in ω and explains the relatively high values of the degree of ionization $N_e/N > 10^{-4}-10^{-3}$ which were obtained in our calculations and observed experimentally in fields in the microwave range.

In addition, it was shown that the propagation of a microwave streamer is accompanied by self-consistent variation of the electron number density in the channel and its spatial dimensions in such a manner that the charge of the plasma channel and the amplitude of the electric field at its center E_0 would vary as little as poissible. It should be stressed that the possibility of utilizing the streamer form of microwave discharges in applications is highly dependent on the strength of this field, since E_0 determines the temperature of the electrons in the stage in which the release of energy in the streamer channel occurs for the most part.

We thank É. M. Bazelyan and Yu. F. Kolesnichenko for their interest in this work and useful discussions.

[1)]It was shown in Refs. 29 and 30 that in a static field the electron number density at the head of a streamer is proportional to its rate of propagation V_c. Therefore, in the absence of preionization, a restriction on the maximal electron number density in the streamer channel follows from the condition that V_c is small in comparison with the velocity of light.

[1] A. Y. Wong, J. Steinhauer, R. Close *et al.*, Comments Plasma Phys. Controlled Fusion **12**, 223 (1989).
[2] G. A. Askar'yan, G. M. Batanov, A. É. Barkhudarov *et al.*, Fiz. Plazmy **18**, 1198 (1992) [Sov. J. Plasma Phys. **18**, 625 (1992)].
[3] V. G. Brovkin, Yu. F. Kolesnichenko, D. B. Khmara, in *Technology. Applied Physics Series* [in Russian], Izd-vo VIMI, Moscow, 1994, Vol. 4, p. 5; N. L. Aleksandrov, S. V. Dobkin, A. M. Konchakov, and D. A. Novitskiĭ, Fiz. Plazmy **20**, 492 (1994) [Plasma Phys. Rep. **20**, 442 (1994)].
[4] V. D. Rusanov and A. A. Fridman, *Phyiscs of Chemically Active Plasmas* [in Russian], Nauka, Moscow, 1984.
[5] Yu. F. Kolesnichenko, in *Radiation-Plasma Methods in Ecology* [in Russian], Izd. MRTI Akad. Nauk SSSR, Moscow, 1989, p. 24.
[6] A. L. Vikharev, V. B. Gil'denburg, and A. V. Kim, in *High-Frequency Discharges in Wave Fields* [in Russian], Izd. Inst. Plazmy Fiz. Akad. Nauk SSSR, Gor'kiĭ, 1988, p. 41.
[7] A. L. Vikharev, A. M. Gorbachev, A. V. Kim, and A. L. Kolysko, Fiz. Plazmy **18**, 1064 (1992) [Sov. J. Plasma Phys. **18**, 554 (1992)].
[8] L. P. Grachev, I. I. Esakov, G. I. Mishin, and K. V. Khodataev, Zh. Tekh. Fiz. **64**, 26 (1994) [Tech. Phys. **39**, 130 (1994)].
[9] S. A. Dvinin, Vestn. Mosk. Univ., Ser. 3: Fiz. Astron. **26**, 30 (1985).
[10] V. B. Gil'denburg, I. S. Gushchin, S. A. Dvinin, and A. V. Kim, Zh. Éksp. Teor. Fiz. **97**, 1151 (1990) [Sov. Phys. JETP **70**, 645 (1990)].
[11] V. G. Avetisov, S. I. Gritsinin, A. V. Kim *et al.*, Pis'ma Zh. Éksp. Teor. Fiz. **51**, 306 (1990) [JETP Lett. **51**, 348 (1990)].
[12] S. I. Gritsinin, A. A. Dorofeyuk, I. A. Kossyĭ, and A. N. Magunov, Teplofiz. Vys. Temp. **25**, 1068 (1987).
[13] V. V. Zlobin, A. A. Kuzovnikov, and V. M. Shibkov, Vestn. Mosk. Univ., Ser. 3: Fiz. Astron. **29**, 89 (1988).
[14] P. S. Bulkin, S. A. Dvinin, G. S. Solntsev, and I. É. Shkradyuk, Vestn. Mosk. Univ., Ser 3: Fiz. Astron. **27**, 15, 1986
[15] L. D. Landau and E. M. Lifshitz, *Electrodynamics of Continuous Media*, Pergamon, Oxford, 1984.
[16] P. V. Vedenin and N. E. Rozanov, Zh. Éksp. Teor. Fiz. **105**, 868 (1994) [J. Exp. Theor. Phys. **78**, 465 (1994)].
[17] A. N. Kolmogorov, *Selected Works of A. N. Kolmogorov. Vol. 1, Mathematics and Mechanics*, Kluwer, Dordrecht, 1991.
[18] I. V. Kochetov, V. G. Pevgov, L. S. Polak, and D. I. Slovetskiĭ, in *Plasma Chemical Processes* [in Russian], Izd. INKhS Akad. Nauk SSSR, Moscow, 1979, p. 4.

[19]N. L. Aleksandrov, F. I. Vysikaĭlo, R. Sh. Islamov *et al.*, Teplofiz. Vys. Temp. **19**, 22 (1981) [High Temp. (USSR) **19**, 17 (1981)].
[20]A. W. Ali, Laser Part. Beams **6**, 105 (1988).
[21]N. A. Dyatko, I. V. Kochetov, and A. P. Napartovich, in *High-Frequency Discharges in Wave Fields* [in Russian], Inst. Plazmy Fiz. Akad. Nauk SSSR, Gor'kiĭ, 1988, p. 9.
[22]I. A. Kossyi, A. Yu. Kostinsky, A. A. Matveev, V. P. Silakov, Plasma Sources **1**, 207 (1992).
[23]N. A. Popov, Teplofiz. Vys. Temp. **32**, 177 (1994) [High Temp. **32**, 166 (1994)].
[24]N. A. Popov, Fiz. Plazmy **20**, 334 (1994) [Plasma Phys. Rep. **20**, 303 (1994)].
[25]A. M. Pravilov, *Photoprocesses in Molecular Gases* [in Russian], Energoatomizdat, Moscow, 1992.
[26]N. A. Bogatov, S. V. Golubev, and V. G. Zorin, Fiz. Plazmy **12**, 1369 (1986).
[27]S. Wang and J. W. McConkey, J. Phys. B **25**, 5461 (1992).
[28]V. A. Shveĭgert, Teplofiz. Vys. Temp. **29**, 227 (1991).
[29]A. É. Bazelyan and É. M. Bazelyan, Teplofiz. Vys. Temp. **32**, 354 (1994) [High Temp. **32**, 332 (1994)].
[30]N. L. Aleksandrov, A. É. Bazelyan, É. M. Bazelyan, and I. V. Kochetov, Fiz. Plazmy **21**, 71 (1995) [Plasma Phys. Rep. **21**, 57 (1995)].

Translated by P. Shelnitz